

RESEARCH ARTICLE

10.1002/2014JD021584

Key Points:

- Combining paleohurricane records and modeling to assess surge risk
- The historical record may greatly underestimate the surge risk
- Assessing the population of storms capable of producing sediment deposits

Supporting Information:

- Readme
- Figures S1–S3

Correspondence to:

N. Lin,
nlin@princeton.edu

Citation:

Lin, N., P. Lane, K. A. Emanuel, R. M. Sullivan, and J. P. Donnelly (2014), Heightened hurricane surge risk in northwest Florida revealed from climatological-hydrodynamic modeling and paleorecord reconstruction, *J. Geophys. Res. Atmos.*, 119, 8606–8623, doi:10.1002/2014JD021584.

Received 29 JAN 2014

Accepted 20 JUN 2014

Accepted article online 26 JUN 2014

Published online 21 JUL 2014

Heightened hurricane surge risk in northwest Florida revealed from climatological-hydrodynamic modeling and paleorecord reconstruction

Ning Lin¹, Philip Lane^{2,3}, Kerry A. Emanuel⁴, Richard M. Sullivan², and Jeffrey P. Donnelly²

¹Department of Civil and Environmental Engineering, Princeton University, Princeton, New Jersey, USA,

²Department of Geology and Geophysics, Woods Hole Oceanographic Institution, Woods Hole, Massachusetts, USA,

³Deceased 11 July 2012, ⁴Department of Earth, Atmospheric, and Planetary Sciences, Massachusetts Institute of Technology, Cambridge, Massachusetts, USA

Abstract Historical tropical cyclone (TC) and storm surge records are often too limited to quantify the risk to local populations. Paleohurricane sediment records uncover long-term TC activity, but interpreting these records can be difficult and can introduce significant uncertainties. Here we compare and combine climatological-hydrodynamic modeling (including a method to account for storm size uncertainty), historical observations, and paleohurricane records to investigate local surge risk, using Apalachee Bay in northwest Florida as an example. The modeling reveals relatively high risk, with 100 year, 500 year, and “worst case” surges estimated to be about 6.3 m, 8.3 m, and 11.3 m, respectively, at Bald Point (a paleorecord site) and about 7.4 m, 9.7 m, and 13.3 m, respectively, at St. Marks (the head of the Bay), supporting the inference from paleorecords that Apalachee Bay has frequently suffered severe inundation for thousands of years. Both the synthetic database and paleorecords contain a much higher frequency of extreme events than the historical record; the mean return period of surges greater than 5 m is about 40 years based on synthetic modeling and paleoreconstruction, whereas it is about 400 years based on historical storm analysis. Apalachee Bay surge risk is determined by storms of broad characteristics, varies spatially over the area, and is affected by coastally trapped Kelvin waves, all of which are important features to consider when accessing the risk and interpreting paleohurricane records. In particular, neglecting size uncertainty may induce great underestimation in surge risk, as the size distribution is positively skewed. While the most extreme surges were generated by the uppermost storm intensities, medium intensity storms (categories 1–3) can produce large to extreme surges, due to their larger inner core sizes. For Apalachee Bay, the storms that induced localized barrier breaching and limited sediment transport (overwash regime; surge between 3 and 5 m) are most likely to be category 2 or 3 storms, and the storms that inundated the entire barrier and deposited significantly more coarse materials (inundation regime; surge > 5 m) are most likely to be category 3 or 4 storms.

1. Introduction

Storm surges and associated waves are responsible for much of the tropical cyclone (TC)-related deaths and damage. Typhoon Haiyan in 2013, the deadliest Philippine typhoon on record, killed more than 6000 people in that country alone, largely due to its storm surge. Storm surge was also a major cause of the over 138,000 fatalities during Cyclone Nargis (2008), the worst natural disaster in Myanmar’s history [Fritz *et al.*, 2009]. Recent U.S. TC surge events include Hurricane Katrina of 2005 in the Gulf of Mexico, which caused over 1800 fatalities and more than \$80 billion in damage [Knabb *et al.*, 2005], and Hurricane Sandy of 2012 on the Northeastern Seaboard, which caused over 70 fatalities and more than \$65 billion in damage [Blake *et al.*, 2013]. As the most fatal and destructive aspect of TCs, storm surges exact a heavy toll on society. Moreover, coastal populations and sea levels are both rising—a combination that ensures that coastal communities will become increasingly vulnerable to storm surges, which themselves may also intensify under the changing climate [Knutson *et al.*, 2010; Mousavi *et al.*, 2011; Lin *et al.*, 2012; Emanuel, 2013; Woodruff *et al.*, 2013]. Mitigation of future TC surge disasters requires us to understand the risk—the scale and probability of TC inundation events.

The main obstacle to assessing the risk is the shortness of the historical/instrumental TC record (over a few decades up to a couple hundred years). As a way to extend the hurricane/typhoon records to prehistory, paleohurricane research has emerged as a promising tool for reconstructing long-term TC activity.

Identifying and dating TC-related deposits in coastal environments makes it possible to estimate the frequencies of intense TCs at a site and determine how they may have evolved over thousands of years [Liu and Fearn, 1993, 2000; Donnelly et al., 2001a, 2001b; Donnelly and Woodruff, 2007; Donnelly and Giosan, 2008; Boldt et al., 2010; Lane et al., 2011; Brandon et al., 2013; van Hengstum et al., 2013]. Such records also provide unprecedented access to natural evidence on hurricane-climate relationships. For example, paleohurricane studies of the U.S. Gulf and East Coasts as well as the Caribbean have identified relatively active and inactive intervals of hurricane activity, which have been tied to climate state variations [Liu and Fearn, 2000; Scileppi and Donnelly, 2007; Donnelly and Woodruff, 2007; Mann et al., 2009; Lane et al., 2011; Brandon et al., 2013; van Hengstum et al., 2013]. Interpretation of these findings is complicated, however, since direct comparison of modern and prehistorical activity is difficult. Event frequencies and return times estimated from sedimentary records generally provide information about the occurrence of extreme surge events on centennial to millennial time scales. Historical records limit analyses to multidecadal or, at best, centennial time scales; extreme and potentially devastating events are rarely documented in the instrumental record.

Historical TC records can also be extended to a millennial time scale (under a stationary climate) through numerical simulations and TC risk modeling [Scheffner et al., 1996; Vickery et al., 2000; Emanuel et al., 2006; Hall and Jewson, 2007; Resio et al., 2009; Toro et al., 2010]. Most of these TC risk models extrapolate the historical TC records, except a statistical-deterministic hurricane risk model [Emanuel et al., 2006], wherein the characteristics of synthetic storms are modeled deterministically by treating the environmental factors that give rise to and affect the evolution of a storm as random variables having values and behaviors consistent with climatology. On the time scale for which accurate meteorological observations are available, the large-scale characteristics of the atmospheric and ocean surface that affect TCs are better constrained than the local or basin-wide distributions of TC characteristics. Modeling the track, intensity, and structure of a very large number of synthetic storms throughout an ocean basin in this way produces a large, representative sample of time-varying realistic storms affecting a region or location of interest. This TC risk model has been integrated with hydrodynamic models into a climatological-hydrodynamic method to estimate local surge risk and applied to New York City [Lin et al., 2010a, 2012]. This method can be applied to any location where ample atmospheric and oceanic data (observed or projected) plus coastal topography and bathymetry information are available. However, as the method aims to estimate the risk beyond the historical TC/surge records, evaluating the method using the historical record is difficult.

A better way to estimate TC surge risk is to apply the climatological-hydrodynamic modeling in conjunction with paleohurricane reconstructions. The climatological-hydrodynamic method provides estimates of surge activity on millennial time scales under modern climate conditions as modern analogs for paleohurricane records. Generating large numbers of synthetic, physically possible storm and surge events, the method also provides constraints on the characteristics of storms capable of inundating a location, allowing investigators to determine characteristics of storms a particular sediment record represents. Meanwhile, the paleohurricane record provides long-term natural evidence to evaluate the climatological-hydrodynamic method, which can generate extremes and event characteristics that are unexpected based on the instrumental record [Lin et al., 2012].

We demonstrate this approach of combining climatological-hydrodynamic modeling and historical and prehistorical records to study surge risk by applying it to the Apalachee Bay area on Florida's Gulf Coast. We extend the climatological-hydrodynamic method of Lin et al. [2012] by incorporating the probabilistic distribution of storm size to account for the uncertainties in size estimation. The storm wind field is greatly affected by the storm size, which may be described by the storm's radius of maximum wind (R_m) and outer radius (R_o ; defined here as the radius at which the wind field becomes indistinguishable from the ambient flow). Thus, storm size critically affects both the magnitude and distribution of surge associated with a storm because the extent of coastal flooding can be very sensitive to the structure of the wind [Fritz et al., 2007; Irish et al., 2008; Lin and Chavas, 2012]. However, no simple physical theory exists for predicting storm size [Rotunno and Emanuel, 1987], and thus, statistical distributions of size may be used when attempting to simulate the full range of events likely to affect a location over a long period. Previous studies [Emanuel et al., 2006; Lin et al., 2012] assumed R_o to be its statistical mean and, with R_o as an input, calculated R_m using a deterministic hurricane model. We develop an empirical relationship to estimate R_m from R_o , which can be determined from its full probability distribution (a lognormal distribution [Chavas and Emanuel, 2010]); thus, probability distributions of both size parameters can be incorporated into the climatological-hydrodynamic method. In addition, we improve the simulation efficiency and accuracy for large sets of surge events by

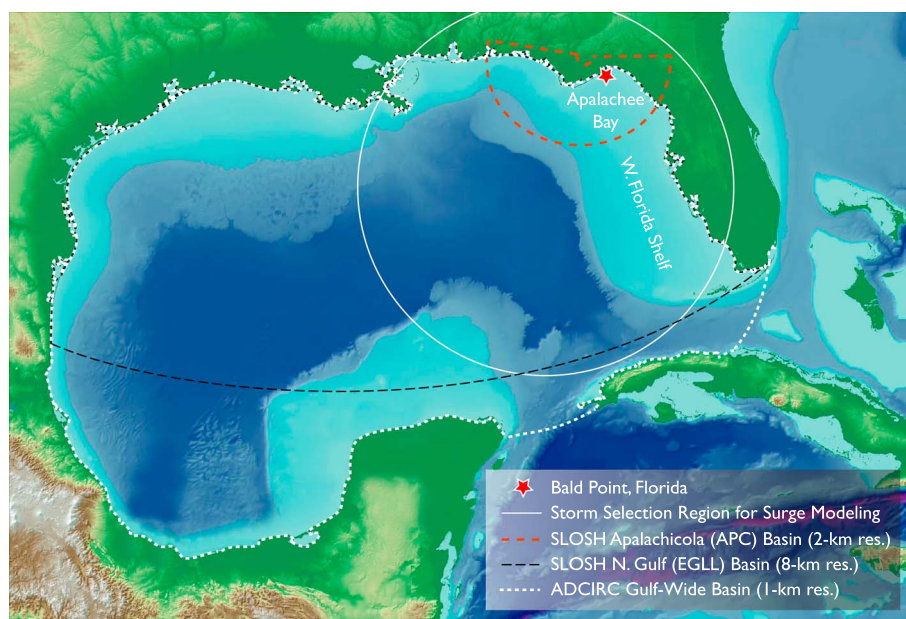


Figure 1. Map of study area, storm selection region, and numerical grids for surge simulations. (The ADCIRC mesh covering the entire Gulf of Mexico with resolution about 1 km around the Apalachee Bay is used to generate all the results presented in the main article.)

applying widely used hydrodynamic models jointly: the Advanced Circulation (ADCIRC) model [Luettich *et al.*, 1992] with a large numerical domain and relatively high resolution is used to generate the surges from significant events (that determine the risk), which are preselected from much larger storm sets by the (computationally more efficient) Sea, Lake, and Overland Surges from Hurricanes (SLOSH) model [Jelesnianski *et al.*, 1992] with various numerical grids and model configurations.

2. Study Site

Apalachee Bay, situated in the Big Bend region of northwest Florida, encompasses 400 km² of the coastal shelf submerged to an average depth of 3 m [U.S. Environmental Protection Agency, 1999] (Figure 1). This shallow, concave bay is highly susceptible to storm surges generated by hurricanes that frequent the Gulf of Mexico. Storm tide-frequency analysis by a joint probability method suggests that the expected maximum 100 year still water level surge in the bay is about 4.5 m [Ho and Tracey, 1975], and inundation modeling indicates that surges exceeding 8 m would penetrate tens of kilometers inland [Jelesnianski *et al.*, 1992]. In addition to its concave geometry and shallow bathymetry, Apalachee Bay is particularly vulnerable to large storm surges due to their enhancement from coastally trapped Kelvin waves. These waves form when storms move northward along Florida's west coast and pile water up along the shelf as they approach the Florida Panhandle. The resulting waves propagate along the coast with the storm and can contribute significantly to the overall surge in Apalachee Bay. For example, Hurricane Kate (1985) and Hurricane Dennis (2005) generated sea height anomalies that propagated along the west Florida shelf and led to a dramatic and unexpected enhancement of the coastal flooding in Apalachee Bay; in each case, the trapped waves contributed an additional meter to the total storm tide in Apalachee Bay [Blain *et al.*, 1994; Morey *et al.*, 2006].

While evidence indicates that Apalachee Bay may be highly vulnerable to hurricane-generated storm surges, tide gauge records in the region are brief and limited (gauges may fail during extreme events) and eyewitness accounts provide evidence for surges no larger than 3–4 m during the historical period [Ludlum, 1963; Case, 1986; Morey *et al.*, 2006]. Analysis of the historical data set reveals that the average return period for a major hurricane (Saffir-Simpson category 3 or greater) landfall in Apalachee Bay (about 73 years) is significantly longer than elsewhere on the U.S. Gulf Coast, which may suggest that the region is in some way sheltered from intense hurricane impacts. However, this stretch of shoreline might simply

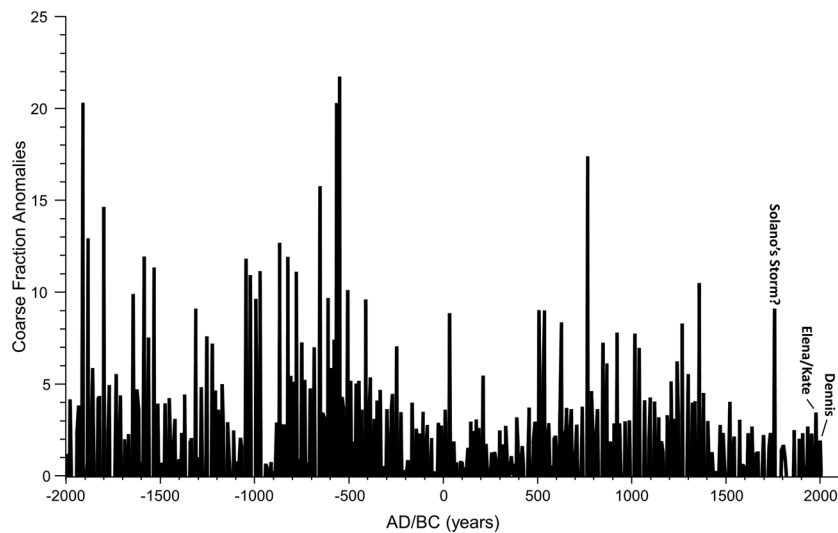


Figure 2. Sediment record reconstruction from Mullet Pond at Bald Point for the last 4000 years [Lane *et al.*, 2011]. Recent historical hurricanes attributable to event beds are noted.

have been fortunate during the approximately 160 years for which historical storm records are available. Thus, paleohurricane records and synthetic climatologies are particularly illuminating in regions such as Apalachee Bay, where vulnerability to the surge may be extreme but observations are brief or otherwise limited.

Our study for this area is further motivated by multimillennial records of extreme inundation obtained from sediment cores collected from coastal sinkholes near Apalachee Bay [Lane *et al.*, 2011; Brandon *et al.*, 2013]. Overwash deposits in the paleorecords show that sites along Apalachee Bay have frequently been subject to marine inundation for at least the last 4000 years (Figure 2). Historical event beds correspond to well documented hurricane-induced flooding events. Tsunamis, another potential mechanism for extreme inundation, have not been historically documented in the Gulf of Mexico. Some have suggested that submarine landslides prior to 7000 years ago may have resulted in tsunamis [Horriillo *et al.*, 2013; ten Brink *et al.*, 2009], but evidence of these types of events has as yet not been uncovered. Thus, the records of marine inundation events recorded in the coastal sinkhole ponds of Apalachee Bay are likely the result of hurricanes. These records suggest that while the frequency of hurricane landfalls in these regions has not changed dramatically over the last several millennia, the frequency of the most intense hurricanes has varied considerably, with intervals of activity of an intensity not seen during the historical period. The current study presents large data sets of surge analysis to help better quantify storm characteristics using the sediment records and provides an estimate of surge activity on millennial time scales under modern climate conditions as a modern analog for the paleohurricane record for Apalachee Bay.

3. Climatological-Hydrodynamic Modeling

The storm surge is a rise of the coastal sea level driven by a storm's surface wind and pressure fields. These fields can be simulated with parametric models, given the storm characteristics including storm track (the movement of the storm), intensity (represented by the storm's maximum wind speed V_m and central pressure deficit ΔP), and size (described by the storm's radius of maximum wind R_m and outer radius R_o). Among these characteristics, size information is often lacking (from both observation and modeling), so we model the size statistically. We model R_o using a lognormal distribution with a mean value of 400 km, based on North Atlantic statistics [Chavas and Emanuel, 2010]. Since R_o is known to vary the least of all hurricane size metrics throughout a storm's lifetime [Frank, 1977], we assume R_o , once sampled from this lognormal distribution, to be a constant over the lifetime of a storm.

We model the evolution of R_m by assuming partial angular momentum conservation of inflowing air as it travels from a storm's outer radius to the radius of maximum wind, based on an analysis of recent

(1988–2006) North Atlantic storm size statistics [Demuth *et al.*, 2006; Kossin *et al.*, 2007]. The R_m evolution at each time step is modeled as follows:

$$V_m R_m + \frac{1}{2} f R_m^2 = \frac{1}{2} \alpha f R_o^2 \quad (1)$$

where f is the latitude-dependent Coriolis parameter and α is the dimensionless fraction of angular momentum that is conserved. Here α is treated as a constant and estimated empirically to be 0.43, the mean value of the solution to the above equation using the Atlantic observations. Note that although it has been shown that there is a near-zero linear correlation between R_m and the radius of the outer closed isobar (similar in magnitude to R_o ; [Carrasco *et al.*, 2014]), R_m and R_o are related through V_m (equation (1)). The modeled R_m distribution (with a mean of 59.7 km) compares well with historical statistics (see Figure S1 in the supporting information). This empirical relationship between R_m and R_o (equation (1)) agrees with an analytical model [Emanuel and Rotunno, 2011], which was used to study the effect on surge risk of the possible change of storm size in a future climate [Lin *et al.*, 2012]. In addition, α can be modeled as a function of latitude so that R_m depends also on the latitude. Compared to a previous model of R_m as a function of intensity and latitude [Vickery *et al.*, 2000], our model is more flexible, depending also on R_o explicitly (the statistics and properties of R_o may be involved, including its possible relationships with the climate environment [Chavas and Emanuel, 2014]).

The generated wind and pressure fields are used to calculate the forces that act upon the ocean's surface, which are applied together with the topography and bathymetry of a coastal region to simulate storm surges using hydrodynamic models. Since surge risk assessment often involves large numbers of simulations and the set of extreme events is always a small fraction, we apply surge simulations with various resolutions to achieve efficiency and accuracy. In this case, we use the relatively low-resolution hydrodynamic model SLOSH with various grid and model configurations to estimate the surge from all the generated storms and select the extreme events for the area. We use the ADCIRC model with a grid of relatively large domain and high resolution to simulate the selected extreme surge events. The selection is sufficient as the SLOSH and ADCIRC model-simulated surges are highly correlated (figure not shown), as also observed previously for the New York area [Lin *et al.*, 2012]. An alternative is to carry out all simulations with only the ADCIRC model using grids of different resolutions. In this study, we chose to use these two hydrodynamic models, both of which are widely used in surge modeling, to also provide an evaluation and comparison between them using large storm sets. The surge modeling method is applicable to both historical and synthetic storm sets.

In this study, we define Apalachee Bay region storms as those that pass within a 500 km radius of a point in the bay (85.58°W, 27.3°N) and have a maximum wind speed of at least 21 m/s, and we focus on these storms in both historical storm database and generated synthetic database. Results are shown in detail for two locations: Bald Point (84.33°W, 29.94°N), near Mullet Pond—the site of the paleohurricane reconstruction [Lane *et al.*, 2011]—and St. Marks (84.18°W, 30.07°N), near the head of Apalachee Bay.

3.1. Historical Storm Analysis

The Atlantic Best-Track data set (also called HURDAT) [Landsea *et al.*, 2004; Landsea and Franklin, 2013] provides positions and maximum wind speed (V_m) at 6 h intervals for historical storms going back to 1851. Of the 1480 North Atlantic storms in the Best-Track data set between 1851 and 2012, 297 (about 20%) meet the proximity and intensity criteria, resulting in a historical annual frequency of 1.84 for Apalachee Bay region storms. We model these 297 storms to estimate the historical surge statistics for the region. As the storm pressure and size information are unavailable for early storms, for consistency, we estimate these quantities empirically for all historical storms. We estimate the barometric pressure difference between the storm center and the ambient environment (ΔP ; the ambient environment pressure is approximated as the global mean sea level pressure) from the Best-Track maximum wind using an empirical wind-pressure relationship specific to the Gulf of Mexico [Landsea *et al.*, 2004]. (A possibly more accurate wind-pressure relationship has been developed [Brown *et al.*, 2006]. Nevertheless, given V_m , uncertainties in ΔP induce relatively small uncertainties in surge estimates.) We assume R_o to be the mean of its distribution (400 km) for each storm and use equation (1) to estimate the value of R_m for each time step during the storm lifetime. To examine the uncertainty in the size estimation, we also treat R_o as a random variable drawn from its lognormal distribution [Chavas and Emanuel, 2010] and carry out another 10 Monte Carlo simulations for each of the 40 Best-Track extreme storms that we focus on (see below about the selection). (Simulated surge heights as a function of R_o for Hurricanes Elena and Kate of 1985 appear in Figure S2 in the supporting information).

3.2. Synthetic Storm Generation

The previously developed statistical-deterministic model [Emanuel *et al.*, 2006, 2008] is used to generate the synthetic storm set. For each storm, a genesis point is generated using a random seeding technique. Once initiated, storm displacements are calculated using the Beta-and-Advection model [Marks, 1992] where 850 and 250 mb environmental steering flows vary randomly but in accordance with their monthly mean, variance, and covariances. The steering flows at these pressure levels are also made to have kinetic energy densities that obey the ω^3 power law of geostrophic turbulence.

The Coupled Hurricane Intensity Prediction System (CHIPS), a deterministic numerical model, is used to simulate the intensity (including V_m and ΔP) of each storm along its simulated track [Emanuel *et al.*, 2004]. The model, which assumes axisymmetric storm structure and includes a one-dimensional ocean, employs climatological values of potential intensity and upper ocean thermal structure to model the intensity evolution of each synthetic storm. It calculates the intensity using an angular momentum coordinate that maximizes model resolution where it is most crucial—in the storm's eyewall. Vertical wind shear, an important factor in the development and intensification of hurricanes, is calculated directly from the modeled steering flows at the 850 and 250 mb pressure levels. The effect of wind shear on storm intensity is accounted for parametrically.

The storm outer radius is drawn from the lognormal distribution with a mean of 400 km, and the storm R_m is calculated using the developed empirical relationship (equation (1)). The statistically modeled synthetic R_m , based on the assumption of partial angular momentum conservation, appears to reasonably replicate the observed relationship between storm intensity and size (see Figure S1 in the supporting information). These generated storm characteristics are then used to simulate storm pressure fields and wind fields (to which an estimated background wind component is added) in the surge modeling.

In this study, we simulate 10,000 synthetic Apalachee Bay region storms, based on the climate conditions of the years 1981–2000 estimated by the National Center for Environmental Prediction/National Center for Atmospheric Research (NCEP/NCAR) reanalysis [Kalnay *et al.*, 1996]. These storms are selected using the Apalachee Bay intensity and proximity criteria from a larger storm set of approximately 52,000 synthetic Atlantic basin storms generated over 5175 years of modeled time, which also implies that about 19% of synthetic Atlantic storms have the potential to impact Apalachee Bay (annual frequency of 1.93).

3.3. SLOSH Surge Simulation

The SLOSH model is an operational, numerical (finite difference) model used by the National Hurricane Center to simulate hurricane storm surges in a time-sensitive, forecast capacity [Jelesnianski *et al.*, 1992]. SLOSH uses a system of polar, hyperbolic, and elliptical grids, called basins. Depending on the basin, the spacing between the model grid points ranges from 0.1 km near the coast to about 7 km in the domain farthest away from the shore. SLOSH also includes parameterizations for some subgrid features, including barriers to flow, breaks in barriers, channel flow, variable friction due to vegetation, and one-dimensional flow in rivers. As such, SLOSH is a nimble but low-resolution model. When compared with higher-resolution models, SLOSH performs well at simulating the maximum storm surge at locations with relatively simple coastal features, though subgrid-scale variations in the local surge will be averaged out [Lin *et al.*, 2010a].

SLOSH applies internal wind and pressure models to generate the wind and pressure fields to drive the surge simulation [Jelesnianski *et al.*, 1992]. Also, it takes the storm pressure deficit ΔP as input (in addition to storm position and size information) and uses an empirical relationship to estimate V_m from the values of ΔP and R_m . This empirical relationship may be invalid, especially for large storms [Jelesnianski *et al.*, 1992], and the information on V_m , even when it is available, is not used. To fully select the extreme events from historical tracks and from our large synthetic database, we applied two techniques: one is to use the observed or simulated ΔP as the input (denoted as useP) and the other is to use a calculated ΔP (denoted as useV) from the inverse of the SLOSH empirical relationship and the (observed or simulated) values of V_m , so that the intensity characteristic actually used is V_m (rather than ΔP).

We also use two different SLOSH simulation domains: the Apalachicola (APC) basin and the Gulf-wide (EGLL) basin (Figure 1). The APC basin has relatively high resolution (about 2 km around Apalachee Bay), but it is small and omits the effects of remotely produced, coastally trapped Kelvin waves, which are sometimes

generated beyond the model domain and can travel into the area of interest. The EGLL basin includes the northern Gulf of Mexico and can simulate the trapped wave phenomenon; however, this basin has much lower resolution (about 8 km around Apalachee Bay). Using these two very different numerical grids further ensures the selection of all extreme events (see Figure S3 in the supporting information).

Thus, we apply the SLOSH simulation to each of the 297 historical and 10,000 synthetic Apalachee Bay region storms 4 times: using the APC basin with useP or useV techniques and using the EGLL basin with useP or useV. We select all storms that generate surges greater than 1.5 m near Bald Point in any of the four cases, resulting in a set of 40 historical and 451 synthetic extreme storm events. The selected synthetic set encompasses events with return periods of about 11 years and longer (in terms of the surge potential at Bald Point), based on the estimated storm frequency. All these selected extreme events are further analyzed with the ADCIRC model.

3.4. ADCIRC Surge Simulation

ADCIRC is a finite element model developed to simulate hydrodynamic circulations along shelves and coasts and within estuaries [Luetlich *et al.*, 1992]. It has been validated and applied to simulate storm surges and make forecasts for various coastal regions [Westerink *et al.*, 2008; Colle *et al.*, 2008; Dietrich *et al.*, 2011; Lin *et al.*, 2010b, 2012; Hope *et al.*, 2013]. The ADCIRC model fully describes the complex physical process associated with storm surge and can also simulate the effects of astronomical tides and wind waves when coupled with a wave model [Dietrich *et al.*, 2011, 2012]. It allows the use of an unstructured grid over a relatively large domain, with very fine resolution near the coast and much coarser resolution in the deep ocean. The high-resolution ADCIRC simulation is computationally intensive, compared to the SLOSH simulation, and thus is not feasible for very large numbers of simulations.

The simulation mesh and the bathymetric data used in this study were previously generated [Blain *et al.*, 1994; Lin and Chavas, 2012]. The mesh covers the entire Gulf of Mexico and has a resolution of approximately 1 km around the Apalachee Bay (Figure 1). The surge simulations can be driven by storm surface wind and sea level pressure fields, which can be generated externally. In our simulations, the surface wind (10 min average at 10 m) is estimated by calculating the wind velocity at the gradient height with an analytical hurricane wind profile [Emanuel and Rotunno, 2011], translating the gradient wind to the surface level with a velocity reduction factor (0.85) [Georgiou *et al.*, 1983] and an empirical expression of inflow angles [Bretschneider, 1972], and adding a fraction (0.55 at 20° counterclockwise) [Lin and Chavas, 2012] of the storm translation velocity to account for the asymmetry of the wind field induced by the surface background wind. These wind parameters are selected based on theories and observations; sensitivities of surge estimates to these parameters were discussed previously [Lin and Chavas, 2012]. The surface pressure is estimated from a parametric pressure model [Holland, 1980]. Other ADCIRC parameters are set to follow a previous study, which were evaluated against observations for the Gulf area [Westerink *et al.*, 2008].

To evaluate our ADCIRC model configuration, we apply it to simulate all historical Apalachee Bay region storms from 1988 to 2012, using the Extended Best-Track data set [Demuth *et al.*, 2006], which includes information on storm track and intensity (as the Best-Track data set) as well as on storm size for this period. There are 47 Apalachee Bay region storms during this period, and our modeling identified significant surges in the Bay induced by Hurricane Allison in 1995 (simulated surge of 2.31 m for Bald Point and 2.59 m for St. Marks), Tropical Storm Josephine in 1996 (1.85 m and 1.82 m), and Tropical Storm Debby in 2012 (1.59 m and 1.55 m). NOAA tidal gauge observations of the water level are available at nearby Apalachicola (84.98°W, 29.73°N) from 1996 (however, the water level during Josephine was not recorded), and the observed surge is estimated as the difference between the observed water level and the predicted astronomical tide. The observed surge for Debby is about 1.09 m, which is close to the simulated value of 1.18 m for Apalachicola. Also, we carried out a survey at Bald Point 12 days after tropical Storm Debby passed to map wrack lines and investigate possible overwash deposits; the observed wrack line elevation is about 1.3 m, which is roughly consistent with the 1.59 m simulated with ADCIRC. Other observations show that the surge in Apalachee Bay was at least 2.1 m for Allison [Lawrence *et al.*, 1998]. Josephine also produced extensive surge flooding from 1.8 to 2.8 m in the eastern Apalachee Bay [Pasch and Avila, 1999]. Our simulations are consistent with these observations; however, our method estimates that the surge from Hurricane Dennis (2005) is less than 1 m, while the observed value is about 2.1 m at the Apalachicola tide gauge, and a storm tide of 3.3 m was noted for Bald Point [Clark and LaGrone, 2006]. Using the storm characteristics and simple parametric wind and pressure profiles caused this underestimation. Close to landfall, the hurricane force winds in Dennis

were localized to near the eye (R_m is only about 9.3 km in the Extended Best Track that we use and about 13 km in the H*Wind surface analysis [Powell *et al.*, 2010]); however, the tropical storm force winds of Dennis extended far eastward over much of the West Florida Shelf, a special feature that may not have been captured by the parametric, symmetric hurricane wind model. When observed wind fields from H*Wind were used, close-to-observed surges were simulated using the SLOSH model [Morey *et al.*, 2006]. Such wind input, however, is unavailable for synthetic storms or earlier historical storms. These comparisons, therefore, show that our ADCIRC configuration can produce relatively accurate surge estimations and that although parametric wind and pressure analysis may be unable to reproduce unusual structures for some storms, they should generate reliable results for long-term climatological analysis and risk estimation.

Thus, this study applies the ADCIRC simulation with this configuration to simulate the storm surge for all the SLOSH-selected extreme historical storms (40 control storms with $R_o = 400$ km as well as 10×40 storms with R_o drawn from its distribution and R_m estimated from equation (1)) and synthetic storms (451 storms with R_o drawn from its distribution and R_m estimated from equation (1); for a comparison, we also simulate the 451 storms with R_o equal to 400 km and R_m estimated deterministically from CHIPS). (See Figure S3 in the supporting information for comparisons between the SLOSH and ADCIRC model simulated surges.) Waves are also simulated for the historical control storms, using the ADCIRC-SWAN-coupled surge-wave model [Dietrich *et al.*, 2011]. The effects of astronomical tides (about ± 0.2 m for the area) are not simulated in this study, as the (statistical) contribution to the risk is relatively small and computationally expensive to account for.

4. Results and Discussion

4.1. Simulated Historical Surges

Among the 297 historical Apalachee Bay region storms (with an annual frequency of 1.84), the SLOSH model simulation selected 40 storms for further analysis with the ADCIRC model. The surge estimation for a particular event is greatly affected by the storm size; the 10 samples of each of the 40 extreme events with R_o drawn from its lognormal distribution vary greatly from the control case (with $R_o = 400$ km; see Figure S2 in the supporting information for examples). Figure 3a shows the histogram of the ratio of the surge of the sample storm and that of the corresponding control storm for all 400 sample events. Assuming the value of R_o to be the distribution mean (the control case) tends to underestimate the surge in the statistical sense, due to the positive skewness of the lognormal distribution of R_o and thus R_m . The propagation of the uncertainties in size estimation to the surge estimation also depends on the local condition: the surge ratio for St. Marks is more positively skewed than that for Bald Point. This complexity induced by storm size in the relationship between storm intensity and surge may explain some of the mismatch between the sediment record and previously simulated historical surge magnitudes [Lane *et al.*, 2011]. Surge risks estimated based on the historical storms are shown in Figure 4 (green curves and color dots) and discussed below, in comparison with the surge risk estimated from the synthetic storms.

Wave simulations show that the wave setup adds negligible amounts to the still water level (surge) at both coastal locations (Figure 3b). The wind waves (on top of the surge) can contribute to run-up, overwash, and the transportation and deposition of sediments. The simulated significant wave height varies almost linearly with the surge height for both locations (Figure 3c). However, the relationship depends on local conditions; wave heights are larger for Bald Point than for St. Marks, although surge heights are smaller for Bald Point. Therefore, wave estimation, in addition to surge estimation, may also be important when interpreting paleosediment records, especially when making intersite comparisons.

4.2. Estimated Surge Risk

Among the 10,000 synthetic Apalachee Bay region storms, the SLOSH model simulation selected 451 synthetic storms for ADCIRC model analysis (with R_o and R_m treated as random variables). The estimated surge risks at Bald Point and St. Marks are shown in terms of the mean return period of the surge height (Figure 4, red curves). The theoretical distribution assumes Poisson arrival of the storms and involves a generalized Pareto distribution to model the surges over a threshold and nonparametric density estimation to model the surges smaller than the threshold [Lin *et al.*, 2010a, 2012]. The estimated 20, 50, 100, 500, 1000, and 5000 year surge levels are about 3.6 m, 5.4 m, 6.3 m, 8.3 m, 9.1 m, and 10.6 m, respectively, for Bald Point, and 4.2 m, 6.3 m, 7.4 m, 9.7 m, 10.6 m, and 12.3 m, respectively, for St. Marks. The “worst surge” is about 11.3 m

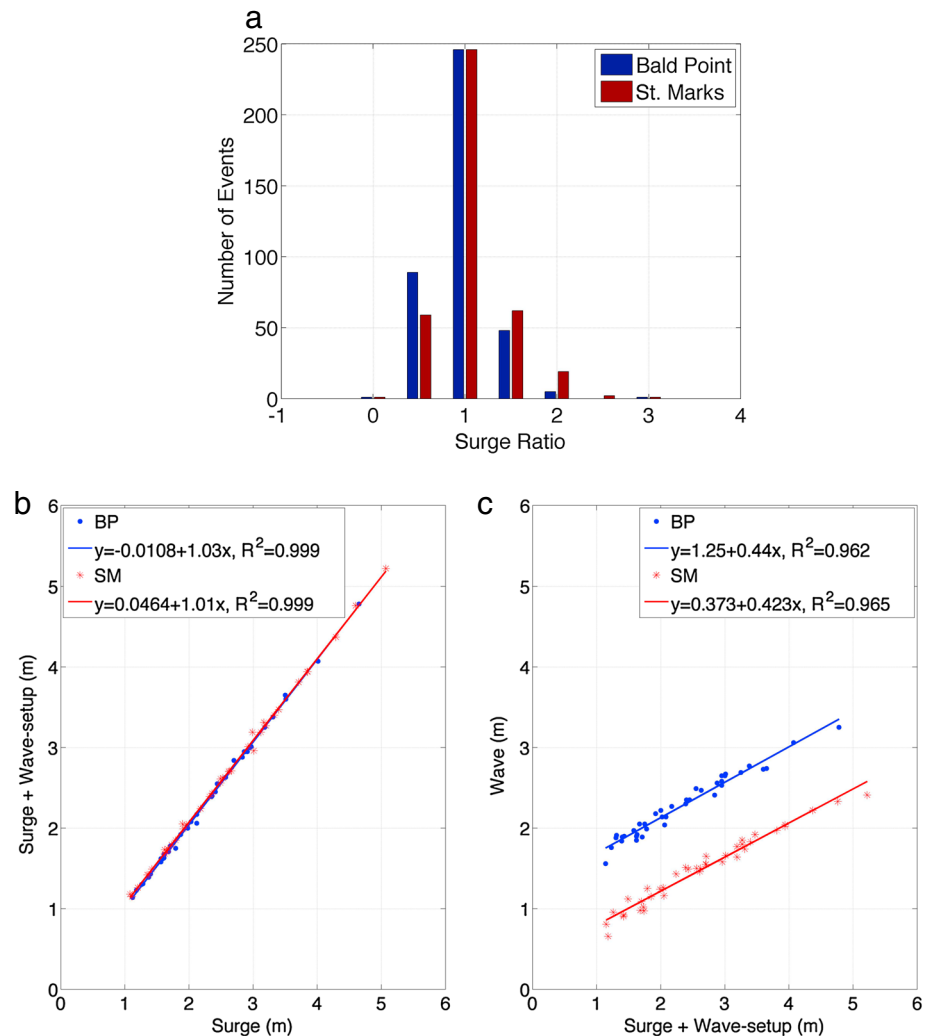


Figure 3. Surge and wave simulations for historical storms. (a) Histogram of the surge ratio (between the sample surge with random size and the control surge with mean size of $R_o = 400$ km) for 10 samples of 40 extreme historical events. (b) The surge height with versus without wave setup (for the control case). (c) The significant wave height versus the surge height (for the control case).

and 13.3 m, for Bald Point and St. Marks, respectively. (It is noted that although these extreme surge levels are much higher than any historical records for Apalachee Bay; they are similar to Hurricane Katrina's surge heights in Mississippi [Fritz *et al.*, 2007].) The spatial variation of the surge level over Apalachee Bay is further shown in Figure 5 for return periods of 500 and 1000 years, as examples, using empirical density estimation at each grid point. These maps reveal the regional distribution of coastal flooding risk. Mapping surge susceptibility in this way reveals that surge climatology can vary dramatically over relatively small distances, controlled primarily by bathymetry, coastline shape, and coastal topography.

As a comparison, the estimated surge risks based on the 451 selected synthetic storms with R_o of 400 km and R_m deterministically estimated from the CHIPS model is also shown (Figure 4, blue curves). Neglecting the size uncertainty may underestimate the surge risk significantly; the estimated 20, 50, 100, 500, 1000, and 5000 year surge levels become about 3.1 m, 4.8 m, 5.5 m, 7.1 m, 7.7 m, and 8.8 m, respectively, for Bald Point, and 3.4 m, 5.8 m, 6.7 m, 8.6 m, 9.3 m, and 10.7 m, respectively, for St. Marks. The worst surge becomes about 9.05 m and 11.4 m, for Bald Point and St. Marks, respectively.

The surge risks estimated from the synthetic storms are also compared with those estimated from the historical storms (Figure 4, green curves and dots for the control historical storms and other color dots for the 10 samples with random R_o and R_m). The estimated 100 year and above surge levels from the synthetic

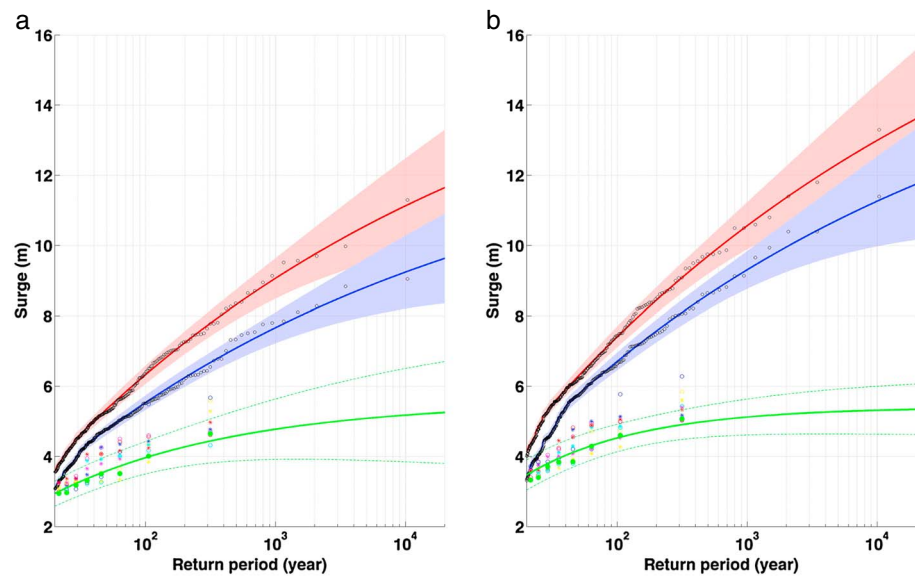


Figure 4. Estimated surge level as functions of return period for (a) Bald Point and (b) St. Marks. The red curve shows the fitted distribution for the synthetic storms with R_o randomly drawn from the lognormal distribution and R_m estimated from their statistical relationship (equation (1)). The blue curve shows the fitted distribution for the synthetic storms with R_o equal to 400 km and R_m estimated from the deterministic CHIPS model. In both cases, the black dots represent the data, and the shade shows the 90% statistical confidence interval. The green solid curve shows the fitted distribution for the historical control storms (R_o equal to 400 km and R_m estimated from equation (1)); the green dots represent the data, and the green-dashed curves show the 90% statistical confidence interval. Other color dots represent the data for the 10 historical storm samples (R_o draw from the lognormal distribution and R_m estimated from equation (1)); fitted distributions for these cases are not shown. Note that the minimum x axis value shown is 20 years, and the minimum y axis value shown is 2 m.

data set (5175 years) are greater than the estimated maximum surge (with size uncertainty accounted for) from the historical data set (161 years from 1851 to 2012) for both sites. The overall storm frequency is only slightly higher in the synthetic set (1.93) than in the historic set (1.84), and frequencies of the surge above small thresholds are similar in the two sets. However, the ratio of surge return period of the historical set over that of the synthetic set increases rapidly with the surge level, about 2 for 4 m and up to 10 for 5 m (based on medium values over the 10 samples of historical storms for both sites). The surge level in the long return period range is much higher for the synthetic set than for the historical set mainly because the

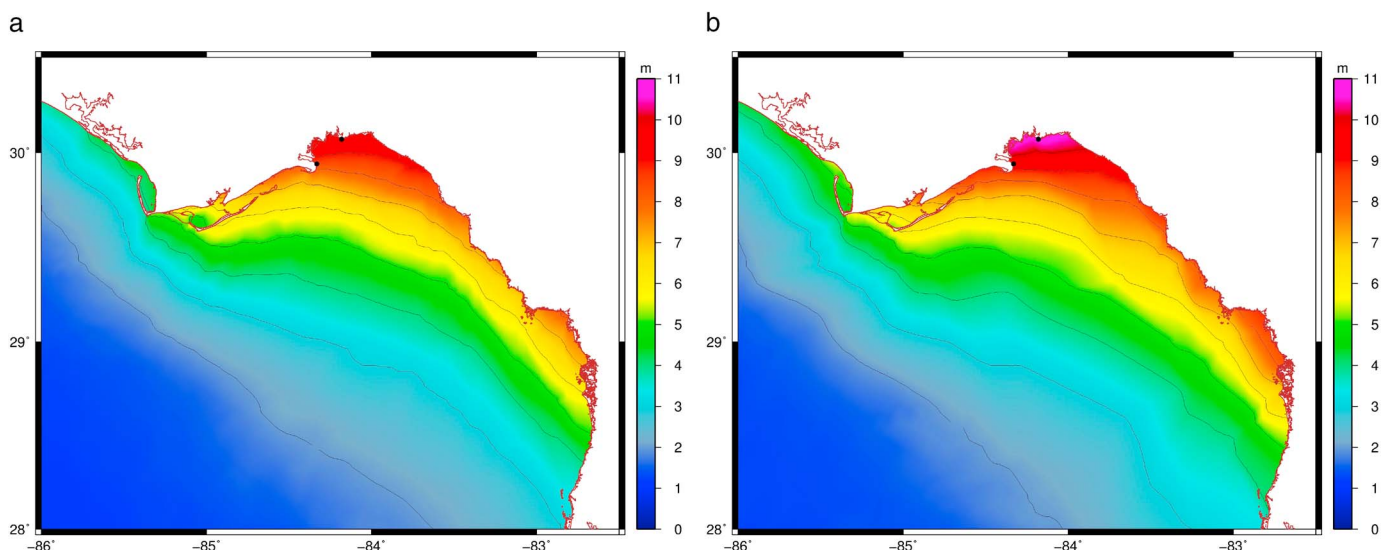


Figure 5. Surge level distribution over Apalachee Bay for (a) 500 and (b) 1000 year return period. The black dots show the location of Bald Point (lower) and St. Marks (upper).

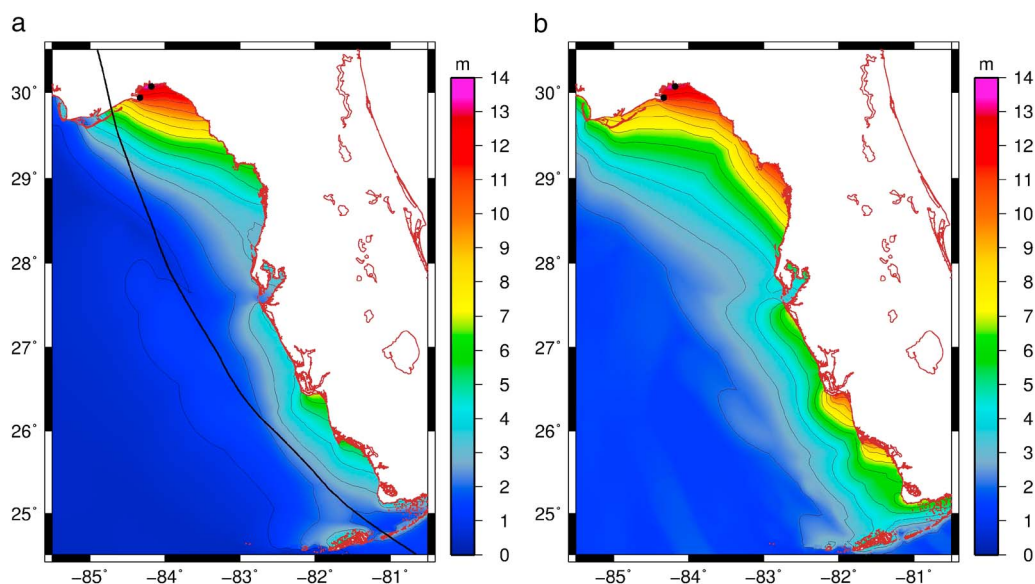


Figure 6. “Worst scenarios” in the synthetic data set. (a) The “worst” surge event (in terms of surge height at Bald Point; the black curve shows the track). (b) The map of the “worst” surge (at each grid point). The black dots show the location of Bald Point (lower) and St. Marks (upper).

synthetic set includes a much larger fraction of intense storms. For example, the frequency of category 4 and 5 storms passing through the Apalachee Bay region is more than twice in the synthetic data set as in the Best-Track record. This may reflect the fact that the storm model was constructed using observations from only the last two decades of the twentieth century (1981–2000), which may have been unusually favorable for North Atlantic hurricane activity compared to the previous decades [Goldenberg *et al.*, 2001]. However, the low frequency of high-intensity historical storms also likely results from the limitations and possible biases of the Best-Track data set for early decades. In the first four decades of the Best-Track data set, only one category 4 storm passed through the search radius of the region, but in the subsequent three 40 year periods 9, 6, and 11 category 4 or 5 storms, respectively, passed through the region. Additionally, no category 5 storms affected the region in the first century in the record, but there were four in the following half century. The mean return period for recorded category 4 and 5 storms after 1960 (1960–2012) is 3.7 years, which is comparable with the synthetically derived return period of 3.1 years (under the climate of 1981–2000). These observations are consistent with previous examinations on the Best-Track data showing that the record for U.S. hurricane strikes is likely only complete since about 1900 (pre-radio) [Landsea *et al.*, 2004] and intense storms are likely undercounted until the 1950s (pre-aircraft reconnaissance) up to 1960s (presatellite) [Hagen and Landsea, 2012]. The analysis result presented here demonstrates the magnitude of errors in surge risk estimation such bias in the historical storm record may induce. It should also be noted that statistically extrapolating limited data to much longer return periods also contributes to the dramatic errors (Figure 4, green curves). Furthermore, the level of extremes in synthetic modeling results are supported by the sediment records (Figure 2) [Lane *et al.*, 2011; Brandon *et al.*, 2013], confirming that relying on the historical records may greatly underestimate the risk of extreme inundation for Apalachee Bay.

The synthetic surges for the modeled 5175 year period include many extremes, unprecedented in the historical record. Of the 10 largest modeled surges at Bald Point, half are category 5 storms at landfall and the other half are category 4 storms, and all these storms originated in the tropical Atlantic Ocean and Caribbean Sea (Main Development Region), traveled westward through the Greater Antilles, and then moved north-northwestward along the west coast of Florida before making landfall near Apalachicola. These storms can trigger coastally trapped Kelvin waves, which may also strongly contribute to the extreme surges. The “worst” surge event—in terms of surge height at Bald Point (11.3 m) among all synthetic events (Figure 6a)—is produced by the combination of, and possibly resonance between, the surge and triggered Kelvin wave propagating along the west Florida shelf. (This event also caused the “worst” surge of 13.3 m for St. Marks.) The “worst” surge map—for each location over all synthetic Apalachee Bay events (Figure 6b)—shows similar high surge patterns along the Florida coast. As the synthetic storms are

generated for the Apalachee Bay region in the northwest Florida, the relatively high water levels they induce along the southwest Florida coast confirms the notion that the Apalachee Bay area is affected by the coastally trapped Kelvin waves. The effect of Kelvin waves may also be affected by the storm size, as large storms that move relatively farther away from the coast can still trigger Kelvin waves. This feature may be considered in interpreting the paleorecords. It also underscores the importance in modeling of using a relatively large numerical domain (including the Florida west coast as the ADCIRC mesh used here) and considering the uncertainty in storm size estimation.

4.3. Sedimentary Record Interpretation

The synthetic hurricane climatology and associated surges combined with historical observations provide essential information for interpreting the sedimentary evidence of past inundation from sites like Mullet Pond at Bald Point (Figure 2). Determining the characteristics of past events from sedimentary deposits can be challenging given that the site configuration and position relative to the shoreline can change with time (see discussion in *Wallace et al.* [2014]). However, assessing the characteristics of recent storms that result in deposition at the site provides a first-order assessment of the sensitivity of the archive to hurricane overwash deposition. The most recent event beds recovered at Mullet Pond correspond in time with Hurricane Dennis in 2005 and Hurricanes Elena and Kate in 1985, providing well-constrained modern analogs for the types of events that are likely recorded in this sediment record. Further, our field survey at Bald Point revealed no evidence of coarse-grained sediment transport to Mullet Pond during Tropical Storm Debby, which thus provides a modern analog for events that are likely not sufficiently intense to be recorded in the sediment archive there.

The highest observed wrack line associated with Debby reached an elevation of approximately 1.3 m above North American Vertical Datum of 1988 (NAVD88). Superimposing those wrack line positions on a LiDAR-based digital elevation model (LiDAR flown September 2010) indicates that Debby-induced floodwaters (approximately 0.6–1.3 m) may have made it into Mullet Pond through inundation of the low-lying salt marsh behind the modern barrier from the north (Figure 7). However, given that the height of the barrier in front of Mullet Pond exceeds 3 m, except for a small inlet about 0.5 km north of the pond, barrier overtopping was not achieved during Debby, so no overwash deposition into Mullet Pond occurred. An inundation event of the scale of Tropical Storm Debby is a typical swash regime event [*Sallenger, 2000*]. In such events, run-up and erosion are confined to the foreshore, and any sediment-transported offshore during the event is typically moved back onshore during subsequent quiescent conditions, resulting in little overall change to coastal geometry. In swash regime, there is typically no transport of sediment to backbarrier environments. In the collision regime [*Sallenger, 2000*], inundation levels reach the base of the dune or barrier ridge, and wave action causes erosion of the seaward margin of the subaerial barrier, but again, no sediment is transported to backbarrier environments.

Observed storm tide elevations at Bald Point were significantly higher relative to NAVD88 for Dennis (3.3 m) [*Clark and LaGrone, 2006*], Elena (2.8 m) [*Bodge and Kriebel, 1985*], and Kate (2.6 m) [*Clark, 1986*] than those of Debby. Based on the 2010 LiDAR survey, the average maximum barrier height fronting Mullet Pond is approximately 4 m above NAVD88, so the barrier was likely not inundated during these events. However, given that offshore significant wave heights for these events were likely between 2.5 and 2.75 m (see Figure 3c), run-up and breaching of lower portions of the barrier probably caused localized overwash and transport of sediment toward into the backbarrier. This local breaching during these events was likely facilitated by perpendicular cuts in the crest of the barrier for driveways of the homes located on the barrier. As the maximum elevation of these driveway cuts is between 3 and 3.5 m above NAVD88, the localized overwash and sediment transport probably occurred through these cuts in Hurricanes Dennis, Elena, and Kate. Consequently, the presence of overwash event layers in the Mullet Pond record associated with these recent storms may have been facilitated by human alteration of the barrier. Nevertheless, it appears that at a minimum, localized breaching of the barrier fronting Mullet Pond is necessary to deposit a detectible coarse-grained event layer in the pond sediments (Figure 7). This type of event is described as an overwash regime [*Sallenger, 2000*], where localized breaching of low areas of the barrier result in overwash and limited transport of sediment in backbarrier environments. Based on the historical documentary records and the inundation modeling presented here, none of the historical surges dating back to the early nineteenth century likely exceeded the height of the modern barrier at Bald Point. Thus, the relatively modest event beds recorded during this recent historical interval likely also resulted during overwash regime events (i.e., localized overwash of the barrier).

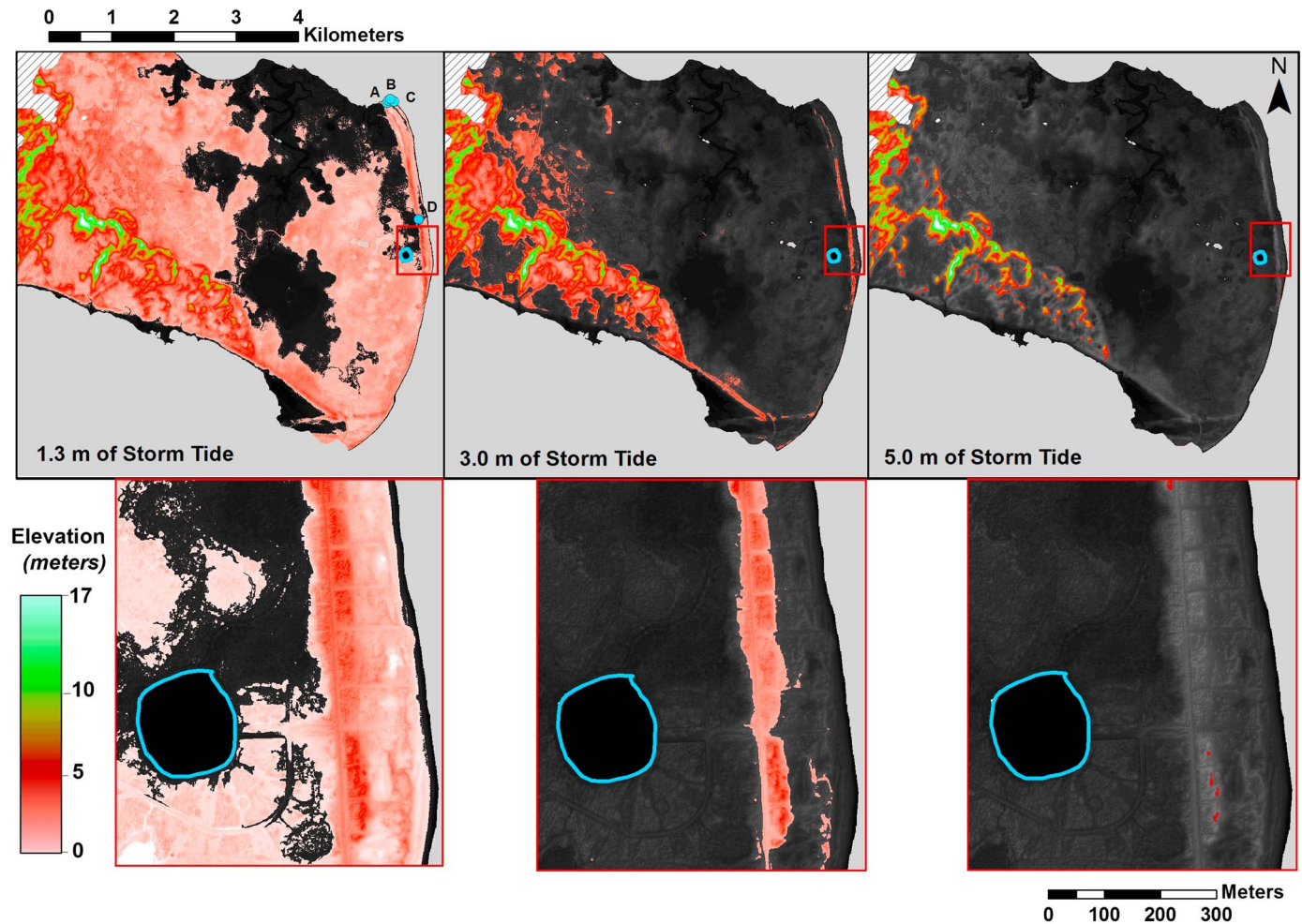


Figure 7. Digital elevation model of Bald Point derived from September 2010 LiDAR survey showing inundation (dark shading) at 1.3 (swash regime), 3.0 (collision/overwash regime), and 5.0 m (inundation regime). Mullet Pond is outlined in light blue and shown in the insets. The locations of mapped wrack lines associated with Tropical Storm Debby are noted in the 1.3 m inundation panel (A = 1.3 m, B = 1.1 m, C = 1.1 m, and D = 0.6 m).

In contrast, many earlier deposits at Mullet Pond contain significantly more coarse material than recent deposits (Figure 2) with the most recent of these dating to the late eighteenth century, possibly related to Solano’s Hurricane in 1780 A.D. [Ludlum, 1963; Lane et al., 2011]. The preservation of these event beds with significantly more coarse material than any of the recent beds suggests more intense hurricanes producing higher levels of surge than those documented historically. Similar results were found in the nearby Spring Creek archive based on the size distribution of particles transported [Brandon et al., 2013]. While changes in site geometry could lead to changes in the sensitivity to overwash through time, the long-term trend should be one of increasing sensitivity as sea level in the northern Gulf of Mexico has gradually risen over the last few millennia [Milliken et al., 2008; Donnelly and Giosan, 2008], causing the shoreline to translate landward toward Mullet Pond. These anomalously large coarse-grained layers were likely transported to the backbarrier ponds during inundation regime events, when the entire barrier was inundated and subjected to surf zone processes [Sallenger, 2000]. During inundation regime events, sheet overwash occurs and sediment can be transported landward more than a kilometer (Figure 7).

Given the modern topography at Bald Point, the site likely transitions into the inundation regime at roughly 5 m of water level rise. Erosion of the barrier during inundation regime is likely to be extensive, and this may result in a site becoming more vulnerable to subsequent flooding events. However, barrier recovery can be quite rapid. For example, foredune elevations recovered at some portions of the Santa Rosa barrier on the Florida Panhandle within a few months of being completely denuded by Hurricane Ivan in 2004 [Wang et al., 2006]. Barrier recovery has been relatively rapid (average rate of 3–4 cm/month) following the

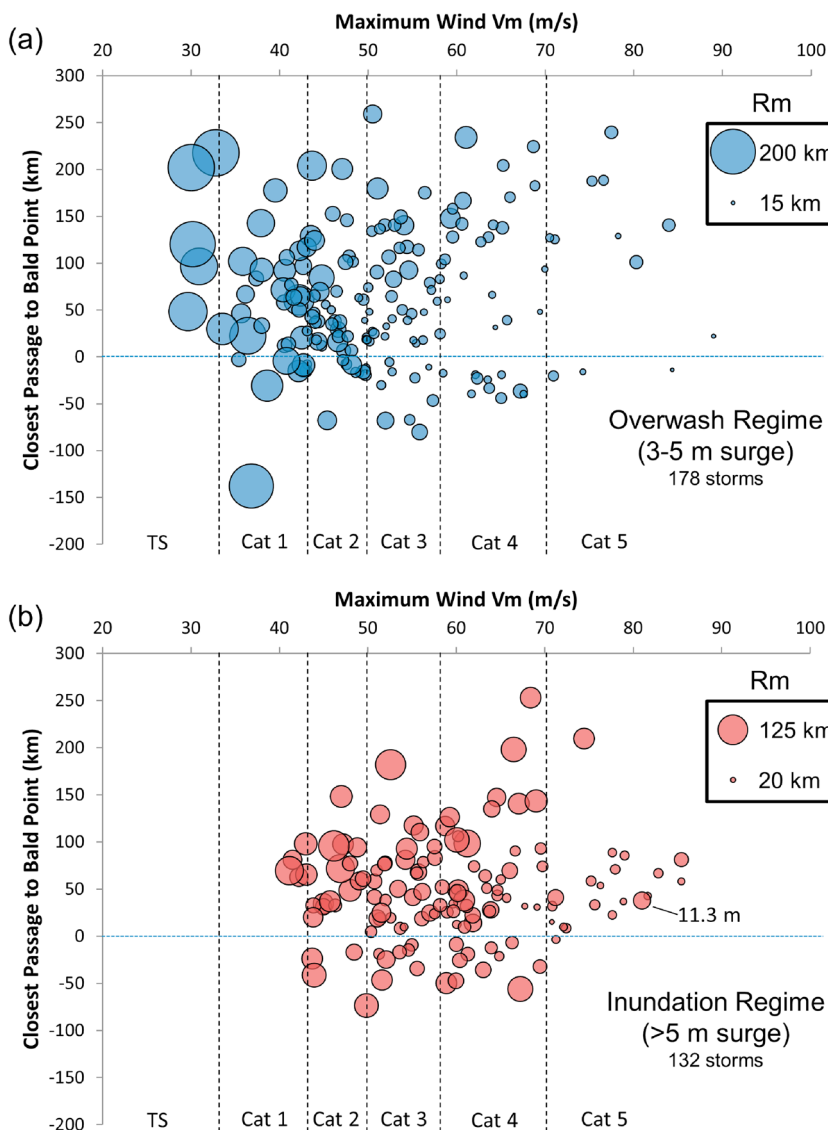


Figure 8. Characteristics of synthetic storms capable of causing overwash and inundation regimes at the Bald Point barrier, from the 451 synthetic storm surge simulations (with R_o randomly drawn). (a) Overwash regime (3 to 5 m of surge). (b) Inundation regime (>5 m of surge). Storm's closest passage to Bald Point is positive if the storm moves to the west of Bald Point and negative if the storm moves to the east of Bald Point. Radius of maximum wind (R_m) is shown with symbol size. Saffir-Simpson categories defined by 1 min maximum sustained winds (V_m) are noted.

removal of the foredune complex at St. George Island (60 km west of Bald Point) during Hurricane Dennis [Priestas and Fagherazzi, 2010]. However, recovery of the barrier to precatastrophic event heights could take years or even decades, depending on subsequent storm frequency and wave climate. Given that the return period for a 5 m surge event from our analysis above is on average roughly 40 years (Figure 4a), similar to the return period of 42 years for overwash layers larger than historically deposited in the 4000 year Mullet Pond archive, the barrier likely has sufficient time to recover between most events. (Note that the analysis based on the historical storm database shows a return period about 10 times longer (about 400 years) for a 5 m surge event; Figure 4a.)

Assuming the modern barrier is a good analog for past barrier geometry, we can examine the population of storms from the synthetic climatology that could produce surges capable of causing overwash regime (3–5 m surge), localized breaching and sediment transport to the backbarrier, as well as inundation regime and sheet overwash (>5 m surge), as shown in Figure 8. It is noted that almost half (49%) of the storms that produced between 3 and 5 m of surge at Bald Point are moderately intense storms (category 2 and weaker;

including 3% from tropical storms) which tend to have relatively large R_m (Figure 8a). An overwash regime storm is more likely to be a category 2 (28%) or category 3 (25%) storm than a category 4 (19%), category 1 (18%), or category 5 (7%) storm. Approximately 78% of the storms resulting in this level of surge passed to the west of Bald Point and 89% passed within 150 km of Bald Point. With 178 events over the 5175 years of modeled time producing 3–5 m of surge, the mean return period for an overwash regime storm at this site is about 29 years.

In the case of hurricanes producing inundation regime events (>5 m of surge; a 40 year event), again assuming modern barrier geometry, the vast majority of storms (82%) are category 3 or greater in intensity (Figure 8b). An inundation regime storm is more likely to be a category 4 (39%) or a category 3 (28%) storm than a category 5 (15%), category 2 (15%), or category 1 (3%) storm. Approximately 83% of the storms resulting in this level of surge passed to the west of Bald Point and 97% passed within 150 km of Bald Point. The worst event for Bald Point, an 11.3 m surge, is associated with an intense (category 5 with sustained winds of 81 m/s) and medium-size (R_m of 71 km) storm that makes landfall closely (30 km) to the west of Bald Point (Figures 8b and 6a). Thus, the vast majority of events in the Mullet Pond archive that deposited more coarse-grained sediment than any recent historically documented hurricane strike were likely deposited in inundation regime surges resulting from the close passage to the west of major hurricanes (category 3 or greater; sustained winds over 50 m/s).

5. Conclusions

Understanding the frequency of hurricane-generated storm surges is a necessary step toward interpreting sediment-based records of hurricane activity and variability as well as quantifying the risk that these events pose to coastal communities. The climatological-hydrodynamic method presented here relates the frequency of surges to their magnitude and provides an estimation of surge flooding risk for Apalachee Bay. The 100 year, 500 year, and “worst case” events are estimated to be about 6.3 m, 8.3 m, and 11.3 m, respectively, at Bald Point and about 7.4 m, 9.7 m, and 13.3 m, respectively, at St. Marks. The results support the notion that this area is extremely susceptible to very large surges capable of completely inundating coastal barriers, producing coarse-sediment event beds in coastal ponds, and penetrating tens of kilometers inland.

Both the climatological-hydrodynamic modeling and the overwash-deposit-based long-term reconstructions indicate that Apalachee Bay is far more susceptible to TC surge than historically observed. The mean return period of the extreme events with estimated surge levels above 5 m is about 40 years in both climatological-hydrodynamic modeling and the geological record, whereas it is about 400 years according to the historical storm database. Thus, due to its limitation and biases, relying on the historical storm record may greatly underestimate the risk of extremes for Apalachee Bay and, likely, for other coastal areas.

Storm size is a critical and uncertain parameter in the climatological-hydrodynamic modeling. Due to the positive skewness of the size metrics, neglecting the size uncertainty may greatly underestimate the surge risk. The size uncertainty may be accounted for using a statistical size model, such as the one developed in this study, which relates radius of maximum wind (R_m) to the storm intensity and outer radius (R_o) and thus involves the probability distributions of R_m and R_o jointly. In addition, the large synthetic data set shows that, for the Apalachee Bay region, significant variability in susceptibility exists over relatively small distances in the area. Thus, relatively high resolution is apparently required for accurate surge simulations over such an area. On the other hand, a large surge model domain is required to adequately simulate the larger-scale effects, such as in this case the coastally trapped Kelvin waves, which often form as storms track northward in this region and can greatly amplify the surge in Apalachee Bay.

While the most extreme surges were generated by the uppermost storm intensities, large surges resulted from a wider range of intensities. Medium-intensity storms (categories 1–3) shoulder a surprising proportion of surge-related risk as they outnumber extremely intense storms and tend to have larger inner wind fields, which can produce higher and more extensive surges than the more compact wind fields of more intense storms. Thus, in addition to storm intensity and track, storm size plays an important role in determining the surge magnitude. This finding implies that it may be difficult to infer the specific paleohurricane intensity from the sedimentary record by constraining the magnitude of the storm surge that produced an overwash deposit. However, the approach presented here provides a means of assessing the population of storms of a variety of intensities, sizes, and tracks that are capable of producing surge levels required to transport coarse-grained barrier and nearshore sediment to coastal ponds and wetlands that preserve a record

of their occurrence. For Bald Point in Apalachee Bay, the majority of the overwash regime storms (surge between 3 and 5 m) are category 2 and 3 storms, and the majority of the inundation regime storms (surge > 5 m) are category 3 and 4 storms. However, the “worst” surges are likely generated by the close passage of category 4 or 5 storms, and some category 1 and even tropical storms with large sizes can also generate significant surges.

The relatively close match between the return period for historically unprecedented overwash event beds determined from the 4000 year paleorecord at Mullet Pond (42 year event) and the return period for inundation regime storms derived from the 5175 year modern synthetic hurricane climatology (40 year event) does not imply that risk of extreme hurricane inundation in Apalachee Bay has been constant over time. Statistically significant clustering of large event beds in the Mullet Pond record [Lane et al., 2011] suggests that changes in global or regional climatic boundary conditions likely played an important role in driving the temporal variation in extreme hurricane inundation over the last several millennia [Lane and Donnelly, 2012; Brandon et al., 2013]. Thus, significant temporal variability in the probability of extreme hurricane-induced inundation has occurred over this interval. In comparison to the last several millennia, the historical interval of the last few hundred years has been anomalously quiescent with respect to the most extreme hurricane-induced inundation events. Applying the climatological-hydrodynamic method to various nonstationary climate conditions, including reconstructed paleoclimates, may shed light on the drivers of the temporal variations of paleohurricane activity.

Acknowledgments

This paper brings to fruition research started by our coauthor and now late colleague and friend, Phil Lane. Phil was a bright and gifted young researcher and our hearts are heavy with his loss. His seemingly limitless potential and passion for studying hurricanes is now lost to the world, and we are certainly worse off for it. Phil was a very kind and giving person with his time and insights, and we take some solace in that his contributions to paleohurricane research will continue to resonate for years to come. This research was funded by National Oceanic and Atmospheric Administration (NOAA) grant NA11OAR4310101 and National Science Foundation (NSF) grants OCE-0903020 and OCE-1250506. The National Center for Airborne Laser Mapping (NCALM) provided the LiDAR data for Bald Point via a Seed grant to P. Lane. We thank Jessica Rodysill and Trevor Harrison, who participated in the post Tropical Storm Debby field survey at Bald Point. We thank the staff at the Bald Point State Park and the Florida State University Marine Lab for their assistance and hospitality.

References

- Blain, C., J. Westerink, and R. Luettich Jr. (1994), The influence of domain size on the response characteristics of a hurricane storm surge model, *J. Geophys. Res.*, *99*(C9), 18,467–18,479.
- Blake, E. S., T. B. Kimberlain, R. J. Berg, P. C. John, and J. L. Beven II (2013), Hurricane Sandy: October 22–29, 2012, *Tropical Cyclone Rep.*, United States National Oceanic and Atmospheric Administration's National Weather Service, Silver Spring, Md.
- Bodge, K. R., and D. L. Kriebel (1985), Storm surge and wave damage along Florida's gulf coast from Hurricane Elena, *Rep. UFL/COEL-85/015*, Coastal and Oceanographic Engineering Department, Univ. of Florida, Gainesville, Fla.
- Boldt, K. V., P. Lane, J. D. Woodruff, and J. P. Donnelly (2010), Calibrating a sedimentary record of overwash from Southeastern New England using modeled historic hurricane surges, *Mar. Geol.*, *275*(1), 127–139.
- Brandon, C. M., J. D. Woodruff, D. Lane, and J. P. Donnelly (2013), Tropical cyclone wind speed constraints from resultant storm surge deposition: A 2500 year reconstruction of hurricane activity from St. Marks, FL, *Geochem. Geophys. Geosyst.*, *14*, 2993–3008, doi:10.1002/ggge.20217.
- Bretschneider, C. (1972), A non-dimensional stationary hurricane wave model, paper presented at Offshore Technology Conference, Paper No. OTC 1517, Houston, Tex.
- Brown, D. P., J. Franklin, and C. Landsea (2006), A fresh look at tropical cyclone pressure-wind relationships using recent reconnaissance based “Best-Track” data (1998–2005), Preprints, paper presented at 27th Conference on Hurricanes and Tropical Meteorology, Am. Meteorol. Soc. B, vol. 3, Monterey, Calif.
- Carrasco, C. A., C. W. Landsea, and Y.-L. Lin (2014), The influence of tropical cyclone size on its intensification, *Weather Forecasting*, *29*, 582–590.
- Case, R. A. (1986), Atlantic hurricane season of 1985, *Mon. Weather Rev.*, *114*, 1390–1405.
- Chavas, D. R., and K. A. Emanuel (2010), A quikscat climatology of tropical cyclone size, *Geophys. Res. Lett.*, *37*, L18816, doi:10.1029/2010GL044558.
- Chavas, D. R., and K. Emanuel (2014), Equilibrium tropical cyclone size in an idealized state of axisymmetric radiative-convective equilibrium, *J. Atmos. Sci.*, *71*, 1663–1680.
- Clark, R., and J. LaGrone (2006), *Hurricane Dennis and Hurricane Katrina: Final Report on 2005 Hurricane Season Impacts to Northwest Florida*, Florida Dept. of Environmental Protection, Division of Water Resource Management, Bureau of Beaches and Coastal Systems, Tallahassee, Fla.
- Clark, R. H. (1986), *Hurricane Kate, November 15–23, 1985*, Dept. of Natural Resources, Division of Beaches and Shores, Fla.
- Colle, B. A., F. Buonaiuto, M. J. Bowman, R. E. Wilson, R. Flood, R. Hunter, A. Mintz, and D. Hill (2008), New York City's vulnerability to coastal flooding: Storm surge modeling of past cyclones, *Bull. Am. Meteorol. Soc.*, *89*(6), 829–841.
- Demuth, J. L., M. DeMaria, and J. A. Knaff (2006), Improvement of advanced microwave sounding unit tropical cyclone intensity and size estimation algorithms, *J. Appl. Meteorol. Climatol.*, *45*(11), 1573–1581.
- Dietrich, J., M. Zijlema, J. Westerink, L. Holthuijsen, C. Dawson, R. Luettich Jr., R. Jensen, J. Smith, G. Stelling, and G. Stone (2011), Modeling hurricane waves and storm surge using integrally-coupled, scalable computations, *Coastal Eng.*, *58*(1), 45–65.
- Dietrich, J., S. Tanaka, J. J. Westerink, C. Dawson, R. Luettich Jr., M. Zijlema, L. Holthuijsen, J. Smith, L. Westerink, and H. Westerink (2012), Performance of the unstructured-mesh, SWAN+ ADCIRC model in computing hurricane waves and surge, *J. Sci. Comput.*, *52*(2), 468–497.
- Donnelly, J. P., and L. Giosan (2008), Tempestuous highs and lows in the Gulf of Mexico, *Geology*, *36*(9), 751–752.
- Donnelly, J. P., and J. D. Woodruff (2007), Intense hurricane activity over the past 5,000 years controlled by El Niño and the West African monsoon, *Nature*, *447*(7143), 465–468.
- Donnelly, J. P., S. Roll, M. Wengren, J. Butler, R. Lederer, and T. Webb (2001a), Sedimentary evidence of intense hurricane strikes from New Jersey, *Geology*, *29*(7), 615–618.
- Donnelly, J. P., et al. (2001b), 700 yr sedimentary record of intense hurricane landfalls in Southern New England, *Geol. Soc. Am. Bull.*, *113*(6), 714–727.
- Emanuel, K., and R. Rotunno (2011), Self-stratification of tropical cyclone outflow. Part I: Implications for storm structure, *J. Atmos. Sci.*, *68*(10), 2236–2249.

- Emanuel, K., C. DesAutels, C. Holloway, and R. Korty (2004), Environmental control of tropical cyclone intensity, *J. Atmos. Sci.*, *61*(7), 843–858.
- Emanuel, K., S. Ravela, E. Vivant, and C. Risi (2006), A statistical deterministic approach to hurricane risk assessment, *Bull. Am. Meteorol. Soc.*, *87*(3), 299–314.
- Emanuel, K., R. Sundararajan, and J. Williams (2008), Hurricanes and global warming: Results from downscaling IPCC AR4 simulations, *Bull. Am. Meteorol. Soc.*, *89*, 347–367, doi:10.1175/BAMS-89-3-347.
- Emanuel, K. A. (2013), Downscaling CMIP5 climate models shows increased tropical cyclone activity over the 21st century, *Proc. Natl. Acad. Sci.*, *110*(30), 12,219–12,224.
- Frank, W. M. (1977), The structure and energetics of the tropical cyclone I. Storm structure, *Mon. Weather Rev.*, *105*(9), 1119–1135.
- Fritz, H. M., C. Blount, R. Sokoloski, J. Singleton, A. Fuggle, B. G. McAdoo, A. Moore, C. Grass, and B. Tate (2007), Hurricane Katrina storm surge distribution and field observations on the Mississippi Barrier Islands, *Estuarine Coastal Shelf Sci.*, *74*(1), 12–20.
- Fritz, H. M., C. D. Blount, S. Thwin, M. K. Thu, and N. Chan (2009), Cyclone Nargis storm surge in Myanmar, *Nat. Geosci.*, *2*(7), 448–449.
- Georgiou, P., A. G. Davenport, and B. Vickery (1983), Design wind speeds in regions dominated by tropical cyclones, *J. Wind Eng. Ind. Aerodynamics*, *13*(1), 139–152.
- Goldenberg, S. B., C. W. Landsea, A. M. Mestas-Núñez, and W. M. Gray (2001), The recent increase in Atlantic hurricane activity: Causes and implications, *Science*, *293*(5529), 474–479.
- Hagen, A. B., and C. W. Landsea (2012), On the classification of extreme Atlantic hurricanes utilizing mid-twentieth-century monitoring capabilities*, *J. Clim.*, *25*(13), 4461–4475.
- Hall, T. M., and S. Jewson (2007), Statistical modelling of North Atlantic tropical cyclone tracks, *Tellus A*, *59*(4), 486–498.
- Ho, F. P., and R. J. Tracey (1975), *Storm Tide Frequency Analysis for the Gulf Coast of Florida From Cape San Blas to St. Petersburg Beach*, Silver Spring, Office of Hydrology, National Weather Service.
- Holland, G. J. (1980), An analytic model of the wind and pressure profiles in hurricanes, *Mon. Weather Rev.*, *108*(8), 1212–1218.
- Hope, M., et al. (2013), Hindcast and validation of hurricane IKE (2008) waves, forerunner, and storm surge, *J. Geophys. Res. Oceans*, *118*(9), 4424–4460, doi:10.1002/jgrc.20314.
- Horrillo, J., A. Wood, G.-B. Kim, and A. Parambath (2013), A simplified 3-D Navier-Stokes numerical model for landslide-tsunami: Application to the Gulf of Mexico, *J. Geophys. Res. Oceans*, *118*, 6934–6950, doi:10.1002/2012JC008689.
- Irish, J. L., D. T. Resio, and J. J. Ratcliff (2008), The influence of storm size on hurricane surge, *J. Phys. Oceanogr.*, *38*(9), 2003–2013.
- Jelesnianski, C. P., J. Chen, and W. A. Shaffer (1992), SLOSH: Sea, lake, and overland surges from hurricanes, NOAA Tech. Rep. NWS 48, US Department of Commerce, National Oceanic and Atmospheric Administration, National Weather Service, Silver Spring, Md.
- Kalnay, E., et al. (1996), The NCEP/NCAR 40-year reanalysis project, *Bull. Am. Meteorol. Soc.*, *77*(3), 437–471.
- Knabb, R. D., J. R. Rhome, and D. P. Brown (2005), *Tropical Cyclone Report: Hurricane Katrina, 23–30 August 2005*, National Hurricane Center, Miami, Fla.
- Knutson, T. R., J. L. McBride, J. Chan, K. Emanuel, G. Holland, C. Landsea, I. Held, J. P. Kossin, A. Srivastava, and M. Sugi (2010), Tropical cyclones and climate change, *Nat. Geosci.*, *3*(3), 157–163.
- Kossin, J. P., J. A. Knaff, H. I. Berger, D. C. Herndon, T. A. Cram, C. S. Velden, R. J. Murnane, and J. D. Hawkins (2007), Estimating hurricane wind structure in the absence of aircraft reconnaissance, *Weather Forecasting*, *22*(1), 89–101.
- Landsea, C. W., and J. L. Franklin (2013), Atlantic hurricane database uncertainty and presentation of a new database format, *Mon. Weather Rev.*, *141*(10), 3576–3592.
- Landsea, C. W., C. Anderson, N. Charles, G. Clark, J. Dunion, J. Fernandez-Partagas, P. Hungerford, C. Neumann, and M. Zimmer (2004), The Atlantic hurricane database re-analysis project: Documentation for the 1851–1910 alterations and additions to the Hurdad database, in *Hurricanes and Typhoons: Past, Present and Future*, edited by R. J. Murnane and K.-B. Liu, pp. 177–221, Columbia Univ. Press, Columbia.
- Lane, P., and J. Donnelly (2012), Hurricanes and typhoons: Will tropical cyclones become stronger and more frequent, *PAGES Newsllett*, *20*(1), 32–33.
- Lane, P., J. P. Donnelly, J. D. Woodruff, and A. D. Hawkes (2011), A decadal-resolved paleohurricane record archived in the late Holocene sediments of a Florida sinkhole, *Mar. Geol.*, *287*(1), 14–30.
- Lawrence, M. B., B. Mayfield, L. A. Avila, R. J. Pasch, and E. N. Rappaport (1998), Atlantic hurricane season of 1995, *Mon. Weather Rev.*, *126*(5), 1124–1151.
- Lin, N., and D. Chavas (2012), On hurricane parametric wind and applications in storm surge modeling, *J. Geophys. Res.*, *117*, D09120, doi:10.1029/2011JD017126.
- Lin, N., K. A. Emanuel, J. Smith, and E. Vanmarcke (2010a), Risk assessment of hurricane storm surge for New York City, *J. Geophys. Res.*, *115*, D18121, doi:10.1029/2009JD013630.
- Lin, N., J. A. Smith, G. Villarini, T. P. Marchok, and M. L. Baeck (2010b), Modeling extreme rainfall, winds, and surge from hurricane Isabel, 2003, *Weather Forecasting*, *25*(5), 1342–1361.
- Lin, N., K. Emanuel, M. Oppenheimer, and E. Vanmarcke (2012), Physically based assessment of hurricane surge threat under climate change, *Nat. Clim. Change*, *2*(6), 462–467.
- Liu, K.-b., and M. L. Fearn (1993), Lake-sediment record of late holocene hurricane activities from coastal Alabama, *Geology*, *21*(9), 793–796.
- Liu, K.-b., and M. L. Fearn (2000), Reconstruction of prehistoric landfall frequencies of catastrophic hurricanes in northwestern Florida from lake sediment records, *Quat. Res.*, *54*(2), 238–245.
- Ludlum, D. M. (1963), *Early American Hurricanes, 1492–1870*, vol. 1, Am. Meteorol. Soc., Boston.
- Luettich Jr., R., J. Westerink, and N. W. Scheffner (1992), ADCIRC: An advanced three-dimensional circulation model for shelves, coasts, and estuaries. Report 1: Theory and methodology of ADCIRC-2DDI and ADCIRC-3DL, *Dredging Research Program Tech. Rep. DRP-92-6*, U.S. Army Engineers Waterways Experiment Station, Vicksburg, Miss.
- Mann, M. E., J. D. Woodruff, J. P. Donnelly, and Z. Zhang (2009), Atlantic hurricanes and climate over the past 1,500 years, *Nature*, *460*(7257), 880–883.
- Marks, D. G. (1992), *The Beta and Advection Model for Hurricane Track Forecasting*, US Department of Commerce, National Oceanic and Atmospheric Administration, National Weather Service, National Meteorological Center, Camp Springs, Md.
- Milliken, K., J. B. Anderson, and A. B. Rodriguez (2008), A new composite holocene sea-level curve for the northern Gulf of Mexico, in *Response of Upper Gulf Coast Estuaries to Holocene Climate Change and Sea Level Rise*, edited by J. B. Anderson and A. B. Rodriguez, *Geol. Soc. Am. Spec. Pap.*, *443*, 1–11.
- Morey, S. L., S. Baig, M. A. Bourassa, D. S. Dukhovskoy, and J. J. O'Brien (2006), Remote forcing contribution to storm-induced sea level rise during Hurricane Dennis, *Geophys. Res. Lett.*, *33*, L19603, doi:10.1029/2006GL027021.

- Mousavi, M. E., J. L. Irish, A. E. Frey, F. Olivera, and B. L. Edge (2011), Global warming and hurricanes: The potential impact of hurricane intensification and sea level rise on coastal flooding, *Clim. Change*, 104(3-4), 575–597.
- Pasch, R. J., and L. A. Avila (1999), Atlantic hurricane season of 1996, *Mon. Weather Rev.*, 127(5), 581–610.
- Powell, M. D., et al. (2010), Reconstruction of Hurricane Katrina's wind fields for storm surge and wave hindcasting, *Ocean Eng.*, 37(1), 26–36.
- Prietas, A. M., and S. Fagherazzi (2010), Morphological barrier island changes and recovery of dunes after Hurricane Dennis, St. George Island, Florida, *Geomorphology*, 114(4), 614–626.
- Resio, D. T., J. Irish, and M. Cialone (2009), A surge response function approach to coastal hazard assessment—Part 1: Basic concepts, *Nat. Hazards*, 51(1), 163–182.
- Rotunno, R., and K. A. Emanuel (1987), An air-sea interaction theory for tropical cyclones. Part II: Evolutionary study using a nonhydrostatic axisymmetric numerical model, *J. Atmos. Sci.*, 44(3), 542–561.
- Sallenger Jr., A. H. (2000), Storm impact scale for barrier islands, *J. Coastal Res.*, 16(3), 890–895.
- Scheffner, N. W., L. E. Borgman, and D. J. Mark (1996), Empirical simulation technique based storm surge frequency analyses, *J. Waterway Port Coastal Ocean Eng.*, 122(2), 93–101.
- Scileppi, E., and J. P. Donnelly (2007), Sedimentary evidence of hurricane strikes in Western Long Island, New York, *Geochem. Geophys. Geosyst.*, 8, Q06011, doi:10.1029/2006GC001463.
- ten Brink, U., D. Twichell, P. Lynett, E. Geist, J. Chaytor, H. Lee, B. Buczkowski, and C. Flores (2009), *Regional Assessment of Tsunami Potential in the Gulf of Mexico*, U.S. Geol. Surv. Admin. Rep.
- Toro, G. R., D. T. Resio, D. Divoky, A. W. Niedoroda, and C. Reed (2010), Efficient joint-probability methods for hurricane surge frequency analysis, *Ocean Eng.*, 37(1), 125–134.
- U.S. Environmental Protection Agency (1999), Ecological condition of estuaries in the Gulf of Mexico, *Tech. Rep. EPA 620-R-98-004*, U.S. Environmental Protection Agency, Office of Research and Development, National Health and Environmental Effects Research Laboratory, Gulf Ecology Division, Gulf Breeze, Fla.
- van Hengstum, P. J., J. P. Donnelly, M. R. Toomey, N. A. Albury, P. Lane, and B. Kakuk (2013), Heightened hurricane activity on the Little Bahama Bank From 1350 to 1650 AD, *Cont. Shelf Res.*, doi:10.1016/j.csr.2013.04.032.
- Vickery, P., P. Skerlj, and L. Twisdale (2000), Simulation of hurricane risk in the us using empirical track model, *J. Struct. Eng.*, 126(10), 1222–1237.
- Wallace, D. J., J. D. Woodruff, J. B. Anderson, and J. P. Donnelly (2014), Palaeohurricane reconstructions from sedimentary archives along the Gulf of Mexico, Caribbean Sea and western North Atlantic Ocean margins, *Geol. Soc., London, Spec. Publ.*, 388, SP388-12.
- Wang, P., J. H. Kirby, J. D. Haber, M. H. Horwitz, P. O. Knorr, and J. R. Krock (2006), Morphological and sedimentological impacts of Hurricane Ivan and immediate poststorm beach recovery along the northwestern Florida barrier-island coasts, *J. Coastal Res.*, 22, 1382–1402.
- Westerink, J. J., R. A. Luettich, J. C. Feyen, J. H. Atkinson, C. Dawson, H. J. Roberts, M. D. Powell, J. P. Dunion, E. J. Kubatko, and H. Pourtaheri (2008), A basin-to channel-scale unstructured grid hurricane storm surge model applied to southern Louisiana, *Mon. Weather Rev.*, 136(3), 833–864.
- Woodruff, J. D., J. L. Irish, and S. J. Camargo (2013), Coastal flooding by tropical cyclones and sea-level rise, *Nature*, 504(7478), 44–52.